JOC Article
pubs.acs.org/joc

Decarboxylative Ketone Aldol Reactions: Development and Mechanistic Evaluation under Metal-Free Conditions

Nicole Blaquiere, Daniel G. Shore, Sophie Rousseaux, and Keith Fagnou*

Centre for Catalysis Research and Innovation, Department of Chemistry, University of Ottawa, 10 Marie Curie, Ottawa, ON, K1N 6N5, Canada

keith.fagnou@uottawa.ca

Received May 25, 2009

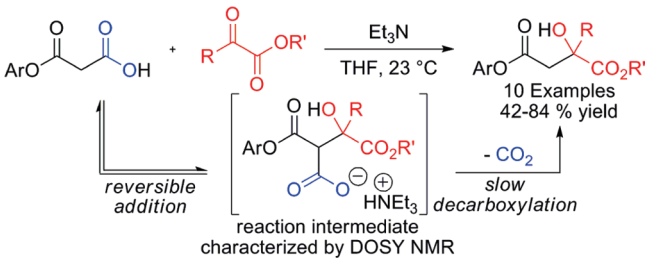

Malonic acid half thioesters (MAHTs) and malonic acid half oxyesters (MAHOs) are shown to undergo decarboxylative nucleophilic addition reactions with ketone and aldehyde electrophiles in the presence of stoichiometric or catalytic quantities of triethylamine at room temperature. The ability to perform these reactions under metal-free conditions has enabled a detailed mechanistic analysis of the reaction pathway leading to the ^{1}H NMR spectroscopic characterization of a postnucleophilic addition/predecarboxylation intermediate and experimental evidence for a reversible formation of this intermediate followed by an irreversible decarboxylation. Rate constants for each of the bond forming/bond breaking steps in the reaction pathway were also determined, casting light on the differing reactivity between MAHO and MAHT nucleophiles in these processes. Finally, the mechanistic insights gained through these studies have been employed in the development of a new decarboxylative coumarin synthesis.

Introduction

Chemists have long drawn inspiration from nature's ability to form carbon−carbon bonds under mild, aqueous, and aerobic conditions. Illustrative are the enzymes that exploit the reactivity of β-ketoacid compounds as a means of facilitating enolate formation such as fatty acid decarboxylase that carries out a chain extension step by the decarboxylative Claisen condensation of malonyl and acetyl units (Scheme 1).[1] The intimate mechanism of these processes remains a matter of debate, with three distinct possibilities being advanced. First, mechanisms involving a concerted decarboxylation and nucleophilic attack have been proposed (mechanism 1, Scheme 1). Alternatively, two stepwise additions have also been proposed, one requiring an initial decarboxylation step to produce a thioester enolate followed

(1) For reviews on polyketide biosynthesis, see: (a) Smith, S.; Tsai, S.-C. *Nat. Prod. Rep.* **2007**, *24*, 1041. (b) Hill, A. M. *Nat. Prod. Rep.* **2006**, *23*, 256. (c) White, S. W.; Zheng, J.; Zhang, Y.-M.; Rock, C. O. *Annu. Rev. Biochem.* **2005**, *74*, 791. (d) Shen, B. *Curr. Opin. Chem. Biol.* **2003**, *7*, 285. (e) Staunton, J.; Weissman, K. J. *Nat. Prod. Rep.* **2001**, *18*, 380.

(2) For references containing evidence supporting a concerted mechanism, see: (a) Cane, D. E.; Liang, T.-C.; Taylor, P. B.; Chang, C.; Yang, C.-C. *J. Am. Chem. Soc.* **1986**, *108*, 4957. (b) Sood, G. R.; Robinson, J. A.; Ajaz, A. A. *J. Chem. Soc., Chem. Commun.* **1984**, 1421. (c) Arnstadt, K. I.; Schindlbeck, G.; Lynen, F. *Eur. J. Biochem.* **1975**, *55*, 561. (d) Vagelos, P. R.; Alberts, A. W. *J. Biol. Chem.* **1960**, *235*, 2786. (e) Brady, R. O. *Proc. Natl. Acad. Sci. U.S.A.* **1958**, *44*, 993. For references that bring additional insight to the accepted concerted mechanism, see: (f) Kresze, G.-B.; Steber, L.; Oesterhelt, D.; Lynen, F. *Eur. J. Biochem.* **1977**, *79*, 191. (g) Lynen, F. *Biochem. J.* **1967**, *102*, 381.

(3) For references containing evidence supporting a stepwise decarboxylation−addition mechanism, see: (a) Davies, C.; Heath, R. J.; White, S. W.; Rock, C. O. *Structure* **2000**, *8*, 185. (b) Dewar, M. J. S.; Dieter, K. M. *Biochemistry* **1988**, *27*, 3302. For references that bring additional insight to the accepted stepwise mechanism, see: (c) Olsen, J. G.; Kadziola, A.; von Wettstein-Knowles, P.; Siggaard-Anderson, M.; Larsen, S. *Structure* **2001**, *9*, 233. (d) Price, A. C.; Choi, K.-H.; Heath, R. J.; Li, Z.; White, S. W.; Rock, C. O. *J. Biol. Chem.* **2001**, *276*, 6551. (e) Jez, J. M.; Ferrer, J.-L.; Bowman, M. E.; Dixon, R. A.; Noel, J. P. *Biochemistry* **2000**, *39*, 890. (f) Dreier, J.; Khosla, C. *Biochemistry* **2000**, *39*, 2088. (g) Qiu, X.; Janson, C. A.; Konstantinidis, A. K.; Nwagwu, S.; Silverman, C.; Smith, W. W.; Khandekar, S.; Lonsdale, J.; Abdel-Meguid, S. S. *J. Biol. Chem.* **1999**, *274*, 36465. (h) Huang, W.; Jia, J.; Edwards, P.; Dehesh, K.; Schneider, G.; Lindqvist, Y. *EMBO J.* **1998**, *17*, 1183. (i) Dewar, M. J. S.; Storch, D. M. *Proc. Natl. Acad. Sci. U.S.A.* **1984**, *82*, 2225.

Published on Web 07/09/2009 DOI: 10.1021/jo901022j

SCHEME 1. Possible Mechanistic Pathways for Enzymatic Decarboxylative Claisen Condensations

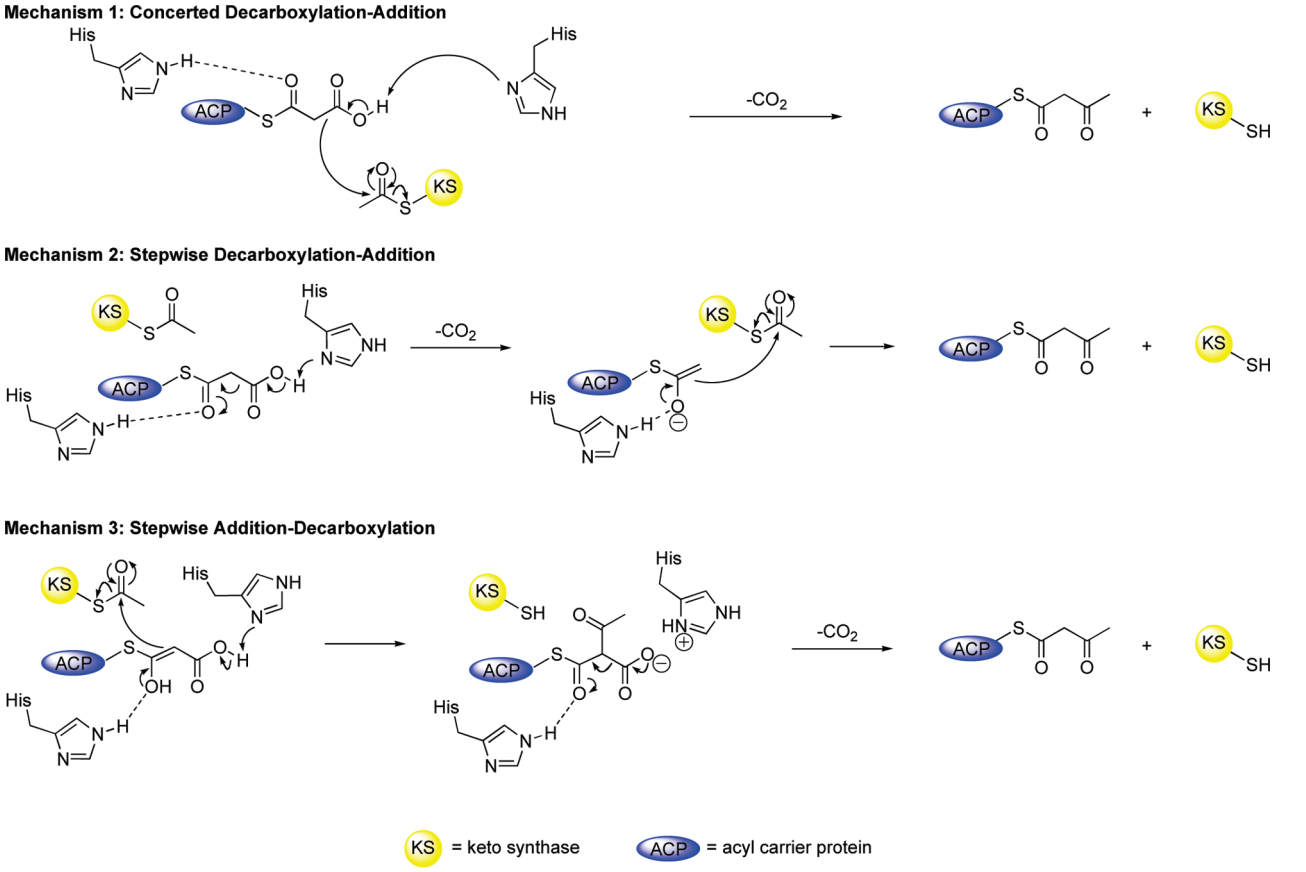

by electrophilic trapping by the acetyl unit (mechanism 2, Scheme 1) and the other involving enolization and nucleophilic addition of the malonyl moiety to the acetyl group followed by decarboxylation (mechanism 3, Scheme 1). There is support for both the concerted (mechanism 1)[2] and the stepwise pathways (mechanisms 2[3] and 3[4]), but a general consensus has not been achieved.

Even in the absence of precise mechanistic knowledge of the discrete reaction steps in biological decarboxylative Claisen condensations, this reactivity has been a source of inspiration for synthetic chemists. For example, in traditional laboratory aldol and related processes, many methods for ester enolate formation involve deprotonation with a strong base followed by trapping as a silyl ketene acetal.[5] A biomimetic approach involving the decarboxylation of half ester malonates can avoid the need for stoichiometric strong bases as well as providing a traceless means of activation with carbon dioxide gas as the only byproduct and providing both enthalpic and entropic driving forces for the global carbon–carbon bond-forming process (Scheme 2).

SCHEME 2. Biomimetic Approach for Laboratory Aldol Processes

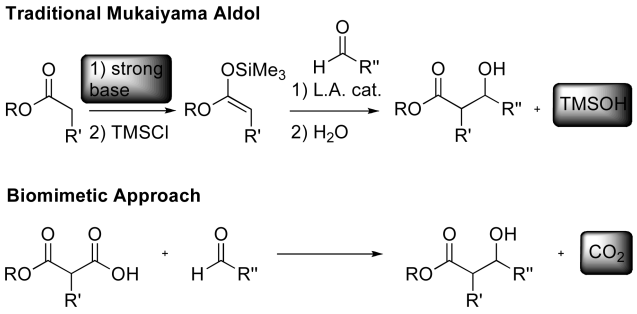

Several transformations have been developed which take advantage of this decarboxylative reactivity,[6,7] the most renowned being the Galat modification of the Knoevenagel–Doebner reaction,[7a] where the decarboxylative addition of malonates to aldehydes results in the formation of

(4) For references containing evidence supporting a stepwise addition–decarboxylation mechanism, see: (a) Sedgwick, B.; Cornforth, J. W. *Eur. J. Biochem.* **1977**, *75*, 465. (b) Vagelos, P. R. *J. Am. Chem. Soc.* **1959**, *81*, 4119. (c) Wakil, S. J.; Ganguly, J. *J. Am. Chem. Soc.* **1959**, *81*, 2597.

(5) For selected reviews, see: (a) Palomo, C.; Oiarbide, M.; García, J. M. *Chem. Soc. Rev.* **2004**, *33*, 65. (b) Palomo, C.; Oiarbide, M.; García, J. M. *Chem.—Eur. J.* **2002**, *8*, 36. (c) Machajewski, T. D.; Wong, C.-H. *Angew. Chem., Int. Ed.* **2000**, *39*, 1352. (d) Mahrwald, R. *Chem. Rev.* **1999**, *99*, 1095. (e) Carreira, E. M. In *Comprehensive Asymmetric Catalysis*; Jacobsen, E. N., Pfaltz, A., Yamammoto, H., Eds.; Springer: Heidelberg, Germany; 1999; Vol. 3, p 997. (f) Nelson, S. G. *Tetrahedron: Asymmetry* **1998**, *9*, 357.

(6) For examples of decarboxylative Claisen condensations, see: (a) Scott, A. I.; Wiesner, C. J.; Yoo, S.; Chung, S.-K. *J. Am. Chem. Soc.* **1975**, *97*, 6277. (b) Kobuke, Y.; Yoshida, J.-I. *Tetrahedron Lett.* **1978**, *4*, 367. (c) Brooks, D. W.; Lu, L. D.-L.; Masamune, S. *Angew. Chem., Int. Ed. Engl.* **1979**, *18*, 72. (d) Sakai, N.; Sordé, N.; Matile, S. *Molecules* **2001**, *6*, 845. (e) Chen, H.; Harrison, P. H. M. *Can. J. Chem.* **2002**, *80*, 601.

(7) For examples of decarboxylative Knoevenagel condensations, see: (a) Galat, A. *J. Am. Chem. Soc.* **1946**, *68*, 376. (b) Ragoussis, N.; Ragoussis, V. *J. Chem. Soc., Perkin Trans. 1* **1998**, 3529. (c) List, B.; Doehring, A.; Hechavarria Fonseca, M. T.; Wobser, K.; van Thienen, H.; Rios Torres, R.; Llamas Galilea, P. *Adv. Synth. Catal.* **2005**, *347*, 1558. (d) Berrué, F.; Antoniotti, S.; Thomas, O. P.; Amade, P. *Eur. J. Org. Chem.* **2007**, 1743.

α,β- and β,γ-unsaturated esters. The concept of decarboxylative enolate addition chemistry has also been investigated by other research groups, including those of Ricci[8] and Wennemers,[9] for additions to imine and nitroolefin electrophiles. Despite the remarkable success associated with this approach, the mechanistic ambiguity associated with the biological processes is mirrored by the uncertainty in the mechanism of the synthetic applications since multiple possibilities (and reactive intermediates) have been advanced across these different reaction classes. In some cases, decarboxylation is proposed to occur prior to nucleophilic attack[6e,8] (analogous to mechanism 2, Scheme 1) and in others, the stepwise nucleophilic addition/decarboxylation mechanism is advanced (analogous to mechanism 3, Scheme 1).[6a,6b,7b,7d]

As direct precedent for the chemistry and the mechanistic work described herein, Shair and co-workers developed both racemic and enantioselective decarboxylative aldol reactions involving the addition of phenyl- and benzylthioesters in the form of malonic acid half thioesters (MAHTs) to a variety of aldehydes in the presence of catalytic copper and a bisoxazolidine ligand (Scheme 3).[10] Cozzi and co-workers have also described an enantioselective decarboxylative aldol reaction between MAHTs and aldehydes using catalytic $Cu(OTf)_2$ and enantiopure bisbenzimidazole ligands.[11]

Mechanistic studies by the Shair group point to the involvement of a stepwise reversible addition of the MAHT to the aldehyde electrophile to form intermediate **1** prior to decarboxylation,[12] analogous to that proposed for the enzymatic process outlined as mechanism 3 in Scheme 1. While intermediate **1** could not be detected directly, indirect evidence for its involvement was obtained from kinetic studies and isotopic labeling experiments. A hypothesis for the role of copper was advanced, involving the enforcement of a planar arrangement of the carboxylate and thioester moieties, stereoelectronically favoring deprotonation over decarboxylation and predisposing the system to follow the stepwise addition/decarboxylation pathway.

The ongoing debate in the literature regarding the mechanism of decarboxylative biological processes and the wide range of proposed pathways for synthetic methods inspired by this reactivity led us to further investigate the mechanism of decarboxylative aldol reactions. Herein we describe (1) the development of amine base-catalyzed decarboxylative aldol reactions between malonic acid half oxyesters (MAHOs) and electron-deficient ketones and aldehydes that occur in the absence of added metal salts (Scheme 4), (2) proof for the involvement of a stepwise addition/decarboxylation pathway (analogous to mechanism 3) by direct observation and characterization of the key postaddition predecarboxylation intermediate in the crude reaction mixture by DOSY ^{1}H NMR, (3) proof for the reversible formation of this postaddition predecarboxylation intermediate based on trapping experiments and kinetic analysis, (4) evidence that the relative rates of each step in the reaction pathway must be considered when developing new reactivity based on this reaction manifold, and (5) use of these findings and validation of their importance in the development of a novel decarboxylative coumarin synthesis from MAHOs and salicylaldehyde substrates. Importantly, these findings may also shed light on the nature of the reaction mechanism in biological systems since, contrary to many previous mechanistic reports,[6a,6b,7d,12] these reactions do not require the presence of a metal catalyst to undergo decarboxylative nucleophilic addition.

SCHEME 3. Copper-Catalyzed Decarboxylative Aldol Reaction with MAHTs

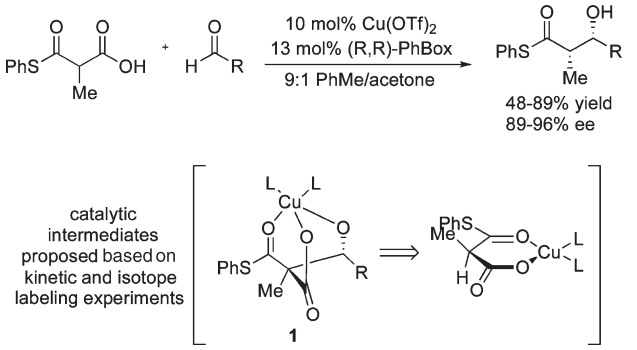

SCHEME 4. Decarboxylative Aldol Reaction between MAHOs and Electron-Deficient Ketones and Aldehydes

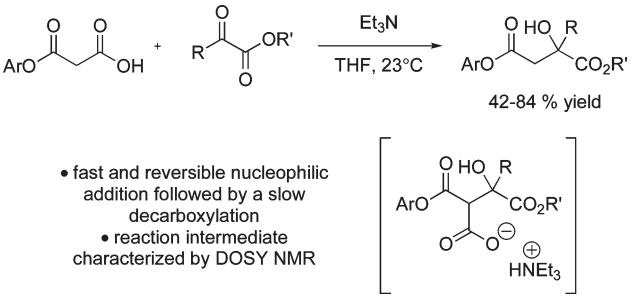

Results and Discussion

To facilitate mechanistic analysis and the detection of reactive intermediates along the reaction pathway by NMR spectroscopy, initial studies targeted the development of metal free decarboxylative aldol condensation reactions. Gratifyingly, it was determined that activated aldehyde and ketone electrophiles, such as ethyl pyruvate, undergo efficient decarboxylative coupling with nucleophiles such as MAHT **2**. For example, in under 3 h, the reaction between MAHT **2** and ethyl pyruvate **4** proceeds smoothly at room temperature in the presence of 1 equiv of triethylamine to afford the β-hydroxythioester **5** in 70% yield (Table 1, entry 1). Catalytic base will also induce decarboxylative addition, with 10 mol % triethylamine resulting in an 86% yield of product overnight (entry 2). Encouraged by this promising reactivity, MAHO **3**, which has not been previously shown to undergo decarboxylative aldol reactions, was also evaluated as a potential coupling partner. We were pleased to see that over a slightly longer reaction time (4 h) and otherwise identical conditions, MAHO **3** also reacts smoothly with ethyl pyruvate (entries 3 and 4).

(8) Ricci, A.; Petterson, D.; Bernardi, L.; Fini, F.; Fochi, M.; Perez Herrera, R.; Sgarzani, V. *Adv. Synth. Catal.* **2007**, *349*, 1037.
(9) Lubkoll, J.; Wennemers, H. *Angew. Chem., Int. Ed.* **2007**, *46*, 6841.
(10) (a) Lalic, G.; Aloise, A. D.; Shair, M. D. *J. Am. Chem. Soc.* **2003**, *125*, 2852. (b) Magdziak, D.; Lalic, G.; Lee, H. M.; Fortner, K. C.; Aloise, A. D.; Shair, M. D. *J. Am. Chem. Soc.* **2005**, *127*, 7284.
(11) Orlandi, S.; Benaglia, M.; Cozzi, F. *Tetrahedron Lett.* **2004**, *45*, 1747.
(12) Fortner, K. C.; Shair, M. D. *J. Am. Chem. Soc.* **2007**, *129*, 1032.

TABLE 1. Optimization of the Decarboxylative Aldol Reaction of Malonic Acid Half Thioesters and Esters with Ethyl Pyruvate[a]

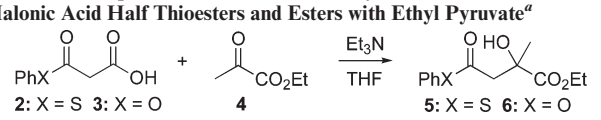

entry	X	Et_3N (equiv)	temp (°C)	yield (%)[b]
1	S	1.0	23	70
2	S	0.1	23	86[c]
3	O	1.0	50	70
4	O	1.0	23	82

[a]Conditions: malonic acid half thioester or oxyester (1 equiv), ethyl pyruvate (1 equiv), triethylamine, THF (0.5 M), 2−4 h. [b]Isolated yields. [c]Overnight reaction.

TABLE 2. Scope of the Decarboxylative Aldol Reaction with MAHO Nucleophiles[a]

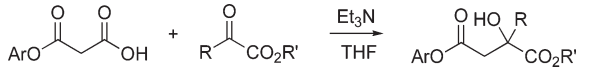

entry	Ar	R	R′	yield (%)[b]
1	Ph	Me	Et	82
2	Ph	CF_3	Et	84
3	Ph	Ph	Et	46
4	Ph	H	Et	65
5	Ph	H	*i*Pr	46
6	Ph	Me	Me	47
7	*p*-CN-C_6H_4	Me	Et	42
8	*p*-F-C_6H_4	Me	Et	70
9	3,5-di(OMe)-C_6H_4	Me	Et	50
10	*p*-OMe-C_6H_4	Me	Et	70

[a]Conditions: malonic acid half oxyester (1 equiv), ethyl pyruvate (1 equiv), triethylamine (1 equiv), THF (0.5), 2−4 h. [b]Isolated yields.

While the reactions can be carried out in the presence of catalytic triethylamine (10 mol %), stoichiometric triethylamine was used in most cases to allow for shorter reaction times. Conveniently, no precautions for the use of inert atmosphere are required since the reactions can be performed at room temperature in an open flask. The reactions proceed well with electron-withdrawing groups on the α-ketoesters (Table 2, entry 2), and also occur with the corresponding phenyl ketone, albeit in lower yields plausibly due to the diminished electrophilicity of this substrate (entry 3). Aldehydes are also compatible, although yields are more variable ranging from 46% to 65% (entries 4 and 5). Distillation of these aldehydes just prior to use was found to be crucial for success since they are known to undergo polymerization at room temperature. Substitution on the aromatic ring of the MAHO with both electron-rich and electron-poor groups also results in moderate to good yields, with electron-rich functionalities generally providing better conversions (entries 7−10). The lower yield in entry 7 may be attributed to the instability of the product due to the heightened electrophilic nature of the ester.[13]

Mechanistic Studies. Crucial to the ability to follow the reaction progress and evaluate the involvement of unstable reactive intermediates is the ability to perform these reactions in the absence of paramagnetic copper(II) salts that can significantly limit the use of NMR spectroscopic analysis of the crude reaction mixture. Employing the newly established reaction conditions and substrate combinations, ^{1}H NMR analysis was performed with a range of substrates. We were pleased to find that ^{1}H NMR analysis of reaction progress between MAHO **3** and ethyl pyruvate **4** with triethylamine-d_{15} in benzene-d_6 revealed the appearance of peaks that were tentatively assigned as the two diastereomers of the postaddition/predecarboxylation intermediate **8** (Figure 1). As might be anticipated, all attempts to isolate this postulated intermediate failed. Consequently, to identify and characterize this intermediate species, DOSY (Diffusion-Ordered SpectroscopY) NMR analysis of the reaction mixture was employed.[14] As shown in Figure 1, unreacted ethyl pyruvate **4** and product **6** can be easily identified.[15] Furthermore, by extracting the peaks that correspond to the third compound in the reaction mixture, this species was identified as the postaddition/predecarboxylation intermediate **8**, providing compelling evidence that the reaction follows a pathway involving a stepwise addition−decarboxylation process (mechanism 3, Scheme 1). While reactions with MAHT substrates proceed too rapidly at room temperature to permit an analogous analysis, by performing the reaction at 0 °C, a similar postaddition/predecarboxylation intermediate could be detected by ^{1}H NMR, supporting a common mechanism for both thioester and ester nucleophiles (Figure 2).

To probe the potential reversibility of the initial addition in this stepwise mechanism, a competition experiment was devised in which a second, and more reactive, electrophile was added to a reaction between MAHO **3** and ethyl pyruvate following maximal conversion to the postaddition/predecarboxylation intermediate **8** (Figure 3). Ethyl trifluoropyruvate was chosen as the second electrophile because of its clean and fast reaction with MAHO **3**[16] along with its structural similarity to ethyl pyruvate. The reaction progress as well as the relative ratios of the unreacted starting materials, the post addition/predecarboxylation intermediate, and the products were monitored by ^{1}H NMR (Figure 3).

To establish baseline reactivity and the optimal moment for the addition of the second electrophile, a kinetic profile for the reaction of MAHO **3** with ethyl pyruvate was obtained. Under standard conditions, maximal conversion (approximately 75%) to the postaddition/predecarboxylation intermediate **8** occurs 130 min into the reaction (Figure 3, solid lines). After 130 min, aldol product **6** is present in 10% yield and 15% of unreacted starting material **3** remains. This point in the reaction profile was chosen for the time of addition of the second electrophile, ethyl trifluoropyruvate, in the competition experiment.

(13) Nonaromatic esters were generally incompatible with the reaction, with only trace amounts of product being observed with malonic acid half ethyl and half *tert*-butyl esters by NMR.

(14) Morris, K. F.; Johnson, C. S. Jr. *J. Am. Chem. Soc.* **1993**, *115*, 4291. This technique is an effective two-dimensional spectroscopic method that permits spectroscopic separation of crude reaction components in a complex mixture according to diffusion constants that depend on variations in size and charge. By extracting horizontal traces from points along the diffusion axis corresponding to the reaction components for a reaction between MAHO **3** (or MAHT **2**) and ethyl pyruvate, structural elucidation of the different species present in the reaction mixture may be achieved.

(15) The diffusion constant for unreacted MAHO **3** is very close to that of intermediate **8**. This made the extraction of a clean ^{1}H NMR spectrum of MAHO **3** from the DOSY spectrum difficult.

(16) See the Supporting Information.

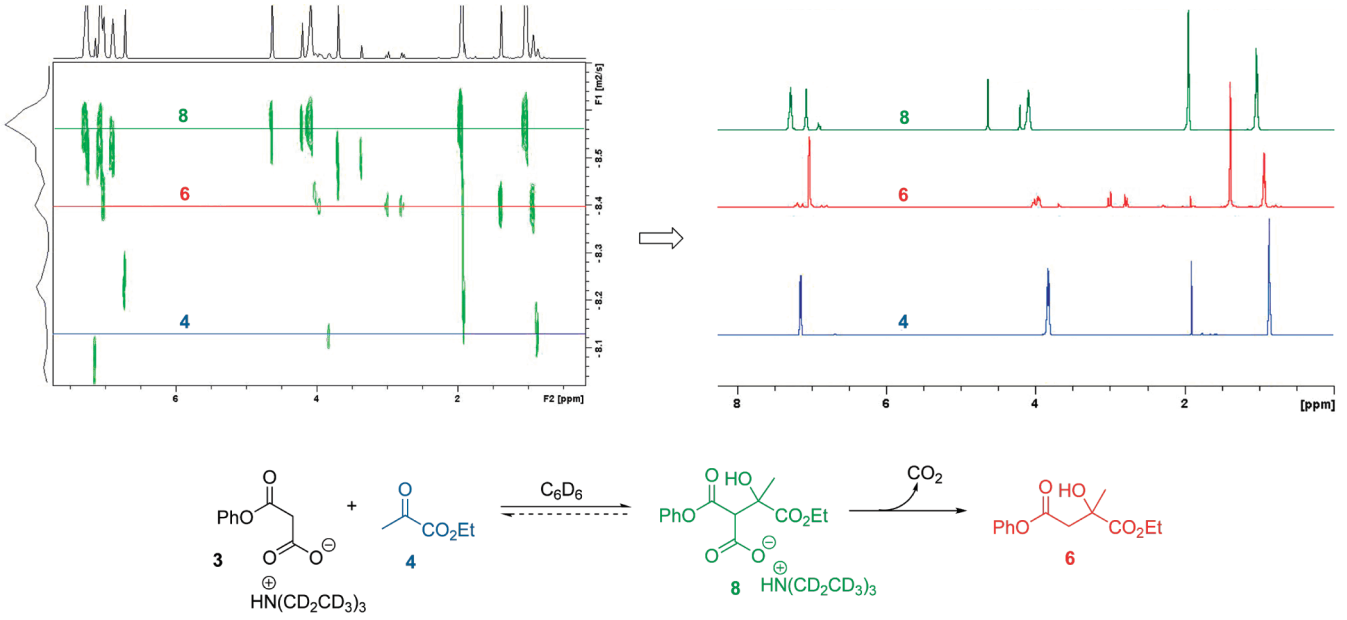

FIGURE 1. DOSY and extracted ^{1}H NMR spectra (500 MHz) of the reaction of MAHO **3** and ethyl pyruvate. For peak assignment of **8**, see the Supporting Information.

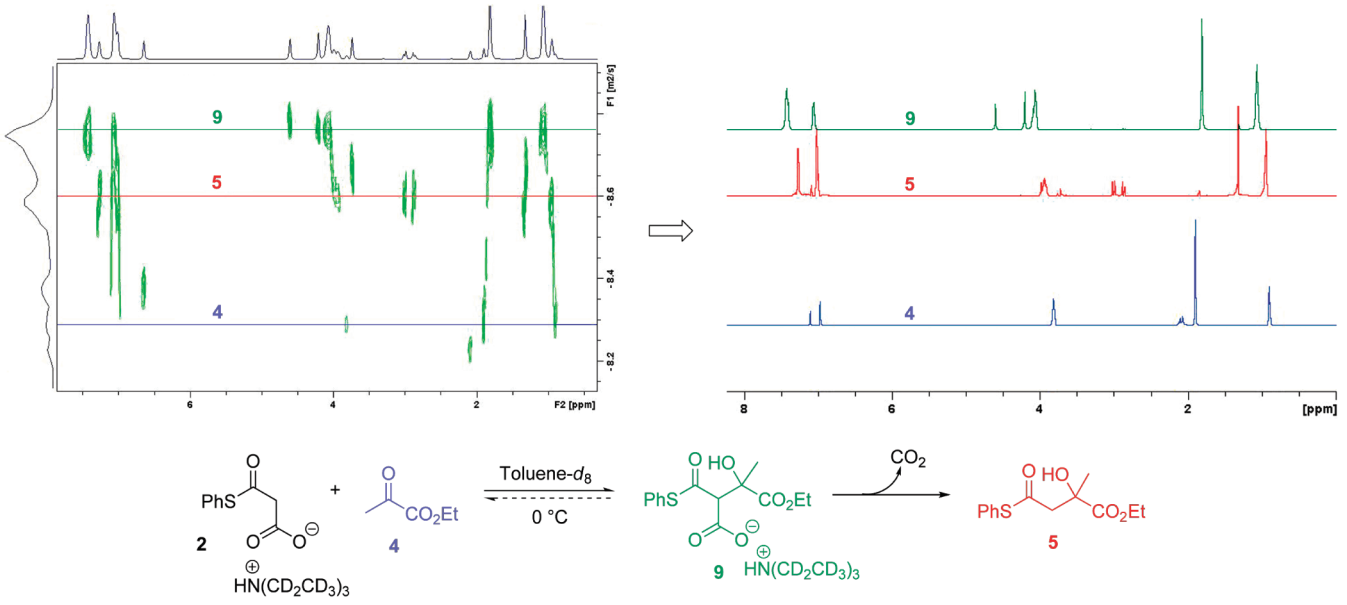

FIGURE 2. DOSY and extracted ^{1}H NMR spectra (500 MHz) of the reaction of MAHT **2** and ethyl pyruvate. For peak assignment of **9**, see the Supporting Information.

A kinetic profile was then obtained for the reaction of MAHO **3** and ethyl pyruvate following the addition of ethyl trifluoropyruvate after 130 min, and a notable diversion from the behavior of the baseline reaction was observed (Figure 3). A significant and rapid drop in MAHO **3** concentration occurs immediately after ethyl trifluoropyruvate addition compared to the baseline reaction due to a fast reaction with this more reactive electrophile. More importantly, a significant decrease in the concentration of intermediate **8** also occurs without concomitant appearance of product **6**. This is a strong indication that, in addition to decarboxylative product formation, there must be another decomposition pathway for intermediate **8**, most likely via a retro-aldol reaction. This would regenerate starting material **3**, which will then undergo fast reaction with the more reactive ethyl trifluoropyruvate to generate a new post addition/predecarboxylation intermediate **10**, and result in a net decrease in the concentration of **8**.

The final product distribution also provides strong evidence for a reversible formation of the postaddition/predecarboxylation intermediate **8**. After 650 min, product **6**, arising from reaction with ethylpyruvate, is formed in 25% yield and **11**, arising from reaction with ethyl trifluoropyruvate, is formed in 41% yield. If the formation of intermediate **8** were irreversible, up to 85% yield of product **6** would be anticipated (resulting from the 75% conversion to intermediate **8** and 10%

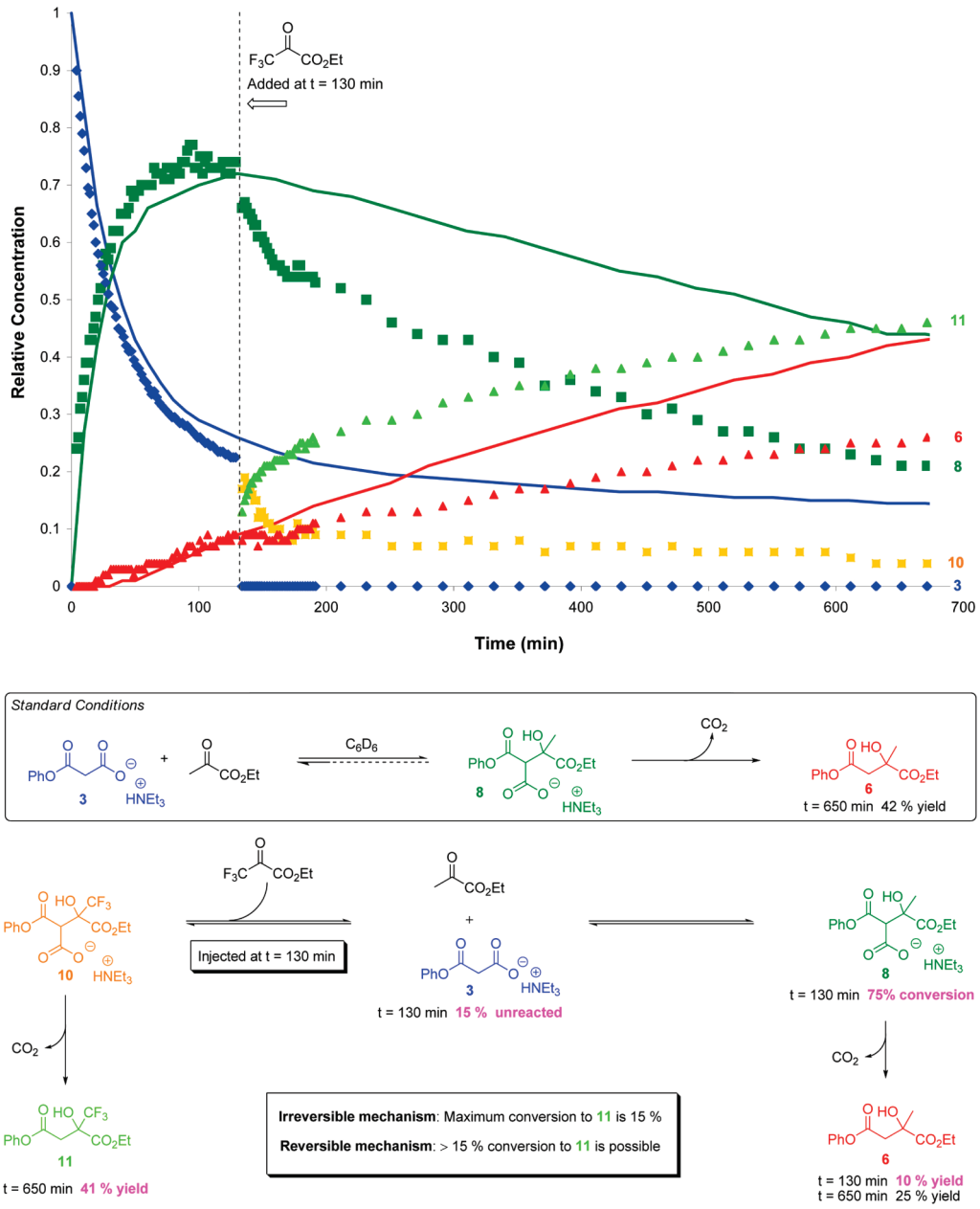

FIGURE 3. Competition experiment between ethyl pyruvate and ethyl trifluoropyruvate electrophiles in the decarboxylative aldol reaction to determine the reversibility of intermediate formation. In the graph, the relative concentrations, monitored by ^{1}H NMR, of MAHO **3**, intermediate **8**, and product **6** under standard conditions (solid lines) are compared to the relative concentrations of the same compounds (blue, dark green, and red data points, respectively) when ethyl trifluoropyruvate is added at 130 min into the reaction. The yellow and light green data points represent the relative concentrations of the newly formed intermediate **10** and product **11** upon addition of this more reactive electrophile. The dashed line represents the time of addition of ethyl trifluoropyruvate.

conversion to product **6** that had occurred prior to addition of the second electrophile), but no more than 15% of **11**, arising from reaction with the second electrophile and unreacted MAHO **3**, could form. Since the experimentally observed yield of **11** surpasses the amount of remaining unreacted **3** at the point of ethyl trifluoropyruvate addition, the difference must be accounted for by a reversion to starting material **3** from the key postaddition/predecarboxylation intermediate **8**, followed by electrophilic trapping by ethyl trifluoropyruvate.

Kinetic Studies. The ability to follow the consumption of starting materials and appearance of the postaddition/predecarboxylation intermediate over time not only allowed for experimental validation of a reversible nucleophilic addition step, but also permits a more detailed kinetic analysis of this reaction pathway casting light on the relative importance of individual steps in the overall process. The integrated rate law of a model system for a reversible addition to the electrophile was evaluated using COPASI (**Co**mplex **Pa**thway **Si**mulator) kinetics analysis software.[17] The second step in the reaction pathway was assumed to be irreversible since

(17) Hoops, S.; Sahle, S.; Gauges, R.; Lee, C.; Pahle, J.; Simus, N.; Singhal, M.; Xu, L.; Mendes, P.; Kummer, U. *Bioinformatics* **2006**, *22*, *3067*. For further information or to download COPASI, see http://www.copasi.org/tiki-index.php.

SCHEME 5. Calculated Rate Constants for the Reversible Reaction of MAHO 3 or MAHT 2 with Ethyl Pyruvate in Benzene-d_6

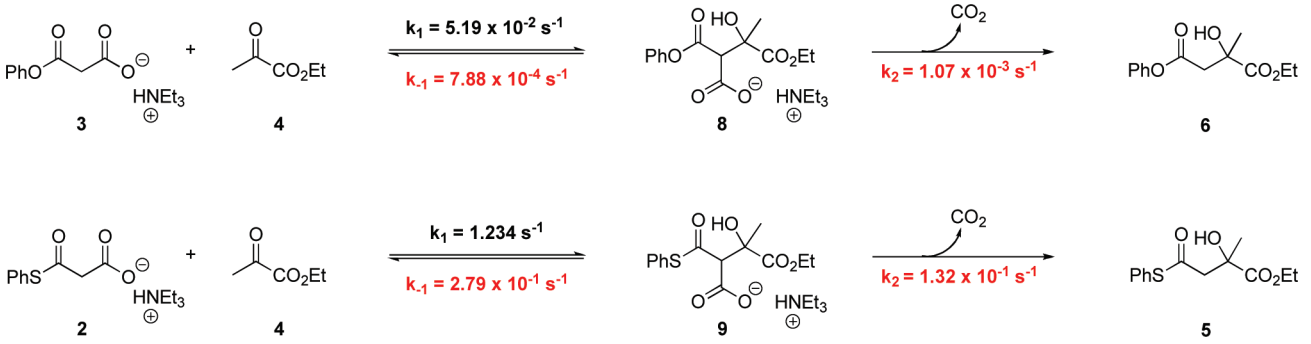

carbon dioxide can bubble out of the reaction and the concentration of CO_2 remaining in the reaction mixture was assumed to be too low to significantly influence the kinetics of the reaction. The integrated rate equation for the reversible model was fit to the experimental data obtained by

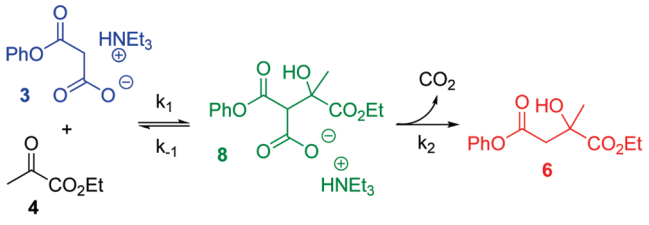

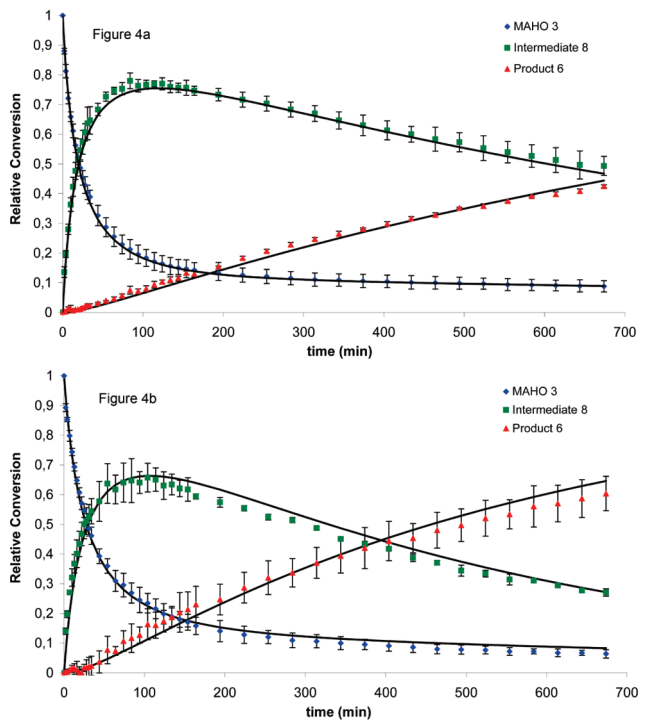

FIGURE 4. Relative concentrations of MAHO **3** (blue), intermediate **8** (green), and β-hydroxyester **6** (red) over 11 h analyzed by ^{1}H NMR in (a) benzene-d_6 and (b) THF-d_8 overlapped with the theoretical curves (solid lines) obtained from the integrated rate equation predicted by COPASI for a reversible mechanism. Data points represent the mean of three trials, and error bars represent the standard deviation. Integrations were measured relative to an internal standard (pentachlorobenzene).

^{1}H NMR analysis of the reaction profile in benzene-d_6 (Figure 4a) and THF-d_8 (Figure 4b) and an excellent accord was observed. The reaction in benzene-d_6 provides a closer fit to the reversible model than the reaction in THF-d_8, which can be explained by the increased amount of side reactions (decarboxylation, etc.) that occur in more polar solvents, affecting starting material concentrations.

The theoretical rate expressions for the reversible model were also solved allowing a determination of the corresponding rate constants (Scheme 5). These values not only point to the important reaction parameters that must be considered during the development of analogous processes, but may also begin to explain the superior reactivity of MAHT compared to MAHO nucleophiles. Reaction with the MAHT nucleophile is associated with faster values for each elemental reaction step. Furthermore, the relative rates for the decarboxylation of intermediates **9**/**8** compared to their formation is larger for MAHT compared to MAHO nucleophiles as well. This agrees with the shape of the plots previously obtained (Figures 3 and 4) where a significant buildup of the postaddition/predecarboxylation intermediate is observed (dark green data points). When envisioning the development of new decarboxylative processes, these results indicate that in addition to the rates of nucleophilic addition, the relative rates of decarboxylation and reversion to starting materials of the first step must be considered. This concept has been illustrated below in the development of a novel decarboxylative coumarin synthesis.

Development of a Decarboxylative Coumarin Synthesis. While evaluating the scope of the amine-catalyzed decarboxylative aldol reactions described herein, it was determined that less reactive carbonyl electrophiles such as benzaldehyde failed to efficiently participate. For example, under standard conditions the addition of MAHO **3** to benzaldehyde results in only 13% yield of the desired aldol product

SCHEME 6. Decarboxylative Aldol Reaction with Benzaldehyde

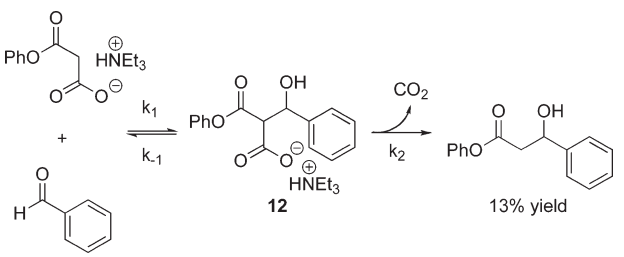

SCHEME 7. Reaction of Salicylaldehyde with MAHO 3

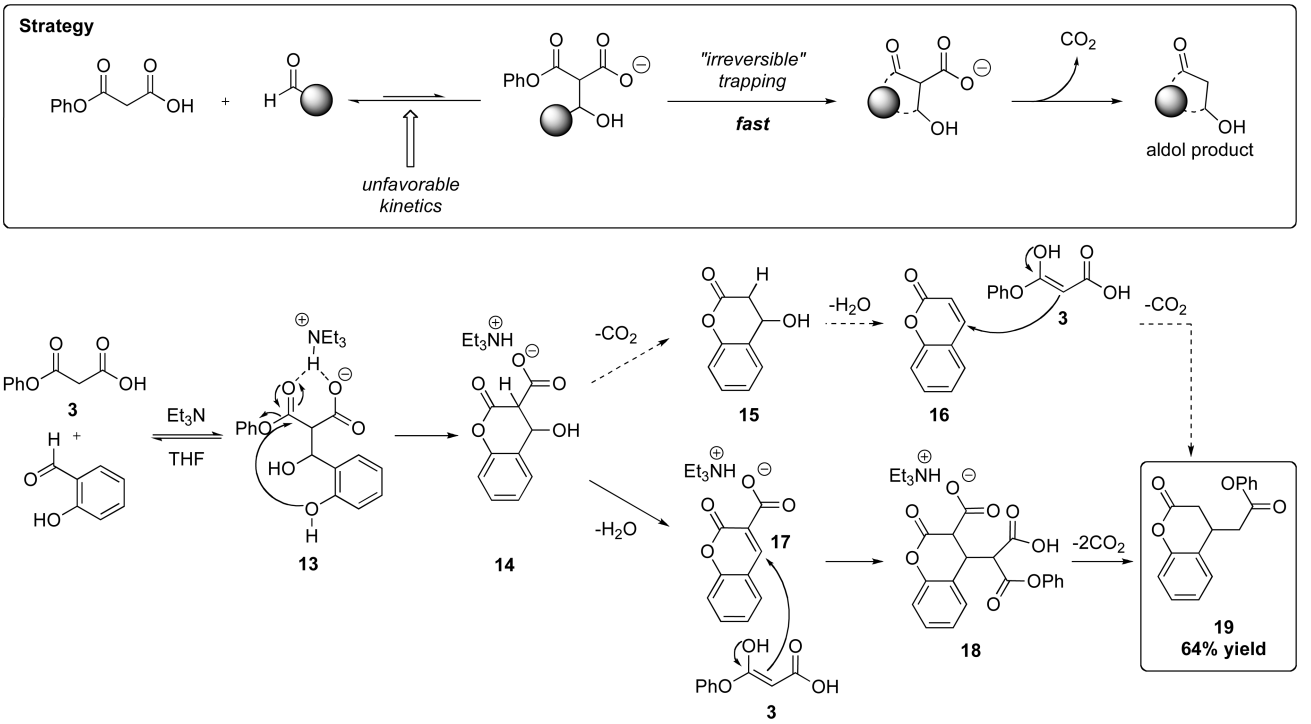

(Scheme 6). Following our mechanistic studies, this was hypothesized as *not only* being a consequence of a slow initial nucleophilic attack (k_1) resulting in low concentrations of intermediate **12**, but perhaps also as a consequence of unfavorable kinetics at the reversible addition (k_{-1}) and decarboxylation steps (k_2). We reasoned that if this intermediate could follow a third reaction pathway that is fast (compared to k_{-1}) and irreversible, then the overall process may become more favorable (Scheme 7).

To test this hypothesis, salicylaldehyde was selected as a suitable electrophile since it was envisioned that upon formation of intermediate **13** (Scheme 7), the *o*-hydroxyl moiety might undergo transesterification with the phenyl ester to give intermediate **14**. Once this has occurred, the retro-aldol step from intermediate **14** would become strongly disfavored thus introducing an alternative "irreversible" step in the overall reaction scheme. A subsequent decarboxylation could then generate coumarin **16**. This notion is supported by the fact that when salicylaldehyde was reacted with 2 equiv of MAHO **3** under the standard reaction conditions,[18] compound **19** was isolated in 64% yield. Subsequent experiments support the involvement of a pathway similar to that depicted in Scheme 7 where dehydration precedes decarboxylation (vide infra). Importantly, the success of this experiment compared to the use of benzaldehyde validates the need to consider all of the reaction steps when proposing the application of this approach in a new process.

To explain the formation of **19** instead of the predicted compound **16**, two additional reactions were carried out. A control reaction between MAHO **3** and coumarin **16** was performed and was found to not result in the formation of **19**, ruling out the possibility of the product arising from 1,4-addition of the malonate to a coumarin intermediate.

(18) Two equivalents of MAHO **3** were used to maximize product yield.

SCHEME 8. Experimental Support for the Proposed Mechanism Outlined in Scheme 6 Where Dehydration Occurs Prior to Decarboxylation

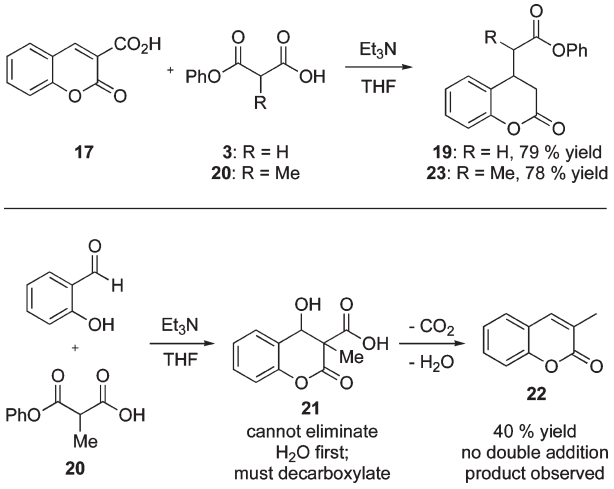

On the other hand, if dehydration were to occur prior to decarboxylation, a new intermediate coumarin-3-carboxylic acid **17** could be formed that might undergo a second reaction with a second MAHO molecule. Consequently, intermediate **17** was synthesized independently, and in the presence of MAHO **3** or **20**, rapidly reacts to give compounds **19** and **23** in good yields (Scheme 8). Finally, reaction of methyl-substituted MAHO **20** with salicylaldehyde provides methyl-substituted coumarin **22** exclusively in 40% yield (Scheme 8). In this instance, the presence of the methyl substituent prevents dehydration prior to decarboxylation at intermediate **21**, leading to the formation of **22**. This novel reaction pathway, and the enhanced reactivity of carboxyl-substituted coumarin **17** compared to **16**, offers a second

useful and conceptually interesting role for the carboxylic acid moiety: in addition to acting as a traceless activating group for the generation of nucleophilic enolates, it may also be used to activate electrophiles in a similar traceless fashion.

Conclusion

In conclusion, an amine base-catalyzed decarboxylative aldol reaction has been developed. Mechanistic studies established the reversible formation of a postaddition/predecarboxylation intermediate in the decarboxylative aldol reaction of both MAHTs and MAHOs. The information garnered from these studies shed light on the importance of considering reversibility and relative rates of elementary reaction steps in reaction development. As well, the application of this decarboxylative reactivity to the synthesis of coumarin derivatives benefited from this mechanistic insight and in turn resulted in the use of the carboxylate moiety as a traceless activating group for the 1,4-addition of malonic acid derivatives to α,β-unsaturated esters. Finally, these mechanistic findings, performed in the absence of metal catalysts and under conditions more closely resembling the biological systems, could influence current opinions as to the pathway of decarboxylative reactions in nature.

Experimental Section

Representative Procedure for the Synthesis of Malonic Acid Half Esters: Monophenyl Malonate (3). A neat solution of 2,2-dimethyl-1,3-dioxane-4,6-dione (5.0 g, 34.7 mmol, 1.0 equiv) and phenol (3.26 g, 34.7 mmol, 1.0 equiv) was heated to 120 °C for 2 h, then cooled to room temperature. The reaction mixture was then concentrated in vacuo and loaded directly on a silica gel column. Chromatography on silica gel (20−40% EtOAc in hexanes) gave 4.7 g of product as a white solid in 75% yield. ^{1}H NMR (300 MHz, $CDCl_3$, 293 K, TMS) δ 3.66 (s, 2H), 7.11−7.14 (m, 2H), 7.22−7.27 (m, 1H), 7.35−7.41 (m, 2H), 8.85 (br s, 1H).

General Procedure for the Decarboxylative Aldol Addition of Malonic Acid Half Esters to Electrophiles: 2-Hydroxy-2-methyl-succinic Acid 1-Ethyl Ester 4-Phenyl Ester (6). Monophenyl malonate (0.100 g, 0.56 mmol, 1.0 equiv) was weighed into a dry screw-capped vial equipped with a magnetic stir bar. THF (1.1 mL, 0.5 M), triethylamine (77 μL, 0.56 mmol, 1.0 equiv), and ethyl pyruvate (62 μL, 0.56 mmol, 1.0 equiv) were added via syringe. The resulting mixture was stirred at room temperature for 4 h, with a hole pierced in the septum to allow release of built up pressure. Upon completion, the solvent was evaporated in vacuo and the reaction mixture was purified by silica gel flash column chromatography (15% EtOAc in hexanes), which afforded 114 mg of product as a clear oil in 81% yield. ^{1}H NMR (400 MHz, $CDCl_3$, 293 K, TMS) δ 1.30 (t, J = 7.5 Hz, 3H), 1.52 (s, 3H), 2.93 (d, J = 16.0 Hz, 1H), 3.22 (d, J = 16.6 Hz, 1H), 3.77 (br s, 1H), 4.22−4.33 (m, 2H), 7.05−7.09 (m, 2H), 7.20−7.26 (m, 1H), 7.35−7.39 (m, 2H). ^{13}C NMR (100 MHz, $CDCl_3$, 293 K, TMS) δ 14.1 (CH_3), 26.5 (CH_3), 44.4 (CH_2), 62.3 (CH_2), 72.5 (C), 121.5 (CH), 126.1 (CH), 129.5 (CH), 150.3 (C), 169.4 (C), 175.4 (C). IR (ν_{max}, cm^{-1}) 3192, 3075, 2936, 1755, 1742, 1592, 1459, 1195, 1115, 759. HRMS calculated for $C_{13}H_{16}O_5$ (M+) 252.0998, found 252.0984.

General Procedure for the Determination of Reaction Profile by ^{1}H NMR. Monophenyl malonate (30 mg, 1.0 equiv) and internal standard pentachlorobenzene (41.7 mg, 1.0 equiv) were weighed into a disposable glass vial. The vial was then charged with 0.75 mL (0.22 M) of deuterated solvent. The reaction mixture was then stirred until homogeneous and the entire solution was transferred by pipet into a clean, oven-dried NMR tube. A baseline ^{1}H NMR spectrum was obtained. All NMR spectra were taken with sample spinning enabled to ensure that the reaction mixture was sufficiently mixed. Et_3N (23 μL, 1.0 equiv) was then added to the NMR tube via syringe, the cap was replaced, and the tube was inverted several times to ensure adequate mixing. A ^{1}H NMR spectrum was then taken to ensure the starting material had been completely deprotonated. Lastly, the electrophile of interest (1.0 equiv) was added via syringe, the time was noted, the tube was inverted to mix, and a starting point ^{1}H NMR spectrum was obtained. The NMR tube cap was replaced with one in which a hole had been pierced to allow the escape of CO_2 gas. Ten ^{1}H NMR spectra were then taken at 1.5 min intervals. Once this program was complete, 20 ^{1}H NMR spectra were taken at 2 min intervals. Upon completion of these spectral scans, spectra were taken at 20−30 min intervals as the sample reacted overnight (8−18 h). Concentrations of reaction components at each time interval were then determined relative to internal standard.

Procedure for the ^{1}H NMR-Monitored Competition Experiment. MAHO **3** (30 mg, 1.0 equiv) and internal standard pentachlorobenzene (41.7 mg, 1.0 equiv) were weighed into a disposable glass vial. The vial was then charged with 0.75 mL (0.22 M) of C_6D_6. The reaction mixture was then stirred until homogeneous and the entire solution was transferred by pipet into a clean, oven-dried NMR tube. A baseline ^{1}H NMR spectrum was obtained. All NMR spectra were taken with sample spinning enabled to ensure that the reaction mixture was sufficiently mixed. Et_3N (23 μL, 1.0 equiv) was then added to the NMR tube via syringe, the cap was replaced, and the tube was inverted several times to ensure adequate mixing. A ^{1}H NMR spectrum was then taken to ensure the starting material had been completely deprotonated. Ethyl pyruvate **4** (1.0 equiv) was added via syringe, the time was noted, the tube was inverted to mix, and a ^{1}H NMR spectrum was obtained. Maximum intermediate concentration is observed at approximately t = 130 min. As such, the NMR tube cap was replaced with one in which a hole had been pierced to allow the escape of CO_2 gas and 10 ^{1}H NMR spectra were taken at 1.5 min intervals. Once this program was complete, ^{1}H NMR spectra were taken at 2 min intervals until t = 130 min. At this point, the second electrophile, ethyl trifluoropyruvate (1.0 equiv), was added via syringe, the tube was inverted, and a starting point ^{1}H NMR spectrum was obtained. Ten ^{1}H NMR spectra were then taken at 1.5 min intervals. Once this program was complete, 20 ^{1}H NMR spectra were taken at 2 min intervals. Upon completion of these spectral scans, spectra were then taken at 20−30 min intervals as the sample reacted overnight (8−18 h). Concentrations of reaction components at each time interval were then determined relative to internal standard.

Acknowledgment. We thank NSERC and the University of Ottawa for support of this work. The Research Corporation, Boehringer Ingelheim (Laval), Merck Frosst Canada, Merck Inc., Eli Lilly, Amgen, and Astra Zeneca Montreal are thanked for additional unrestricted financial support. N. B. thanks NSERC for a postgraduate scholarship (CGS-M), and S.R. thanks NSERC for an undergraduate summer research award. Dr. Glenn Facey is thanked for NMR spectroscopy assistance. Dr. Benoît Liégault is thanked for assistance in preparing several figures.

Supporting Information Available: Detailed experimental procedures for the synthesis of all compounds, characterization data and ^{1}H and ^{13}C NMR spectra for all new compounds, and derivation of the integrated rate laws. This material is available free of charge via the Internet at http://pubs.acs.org.